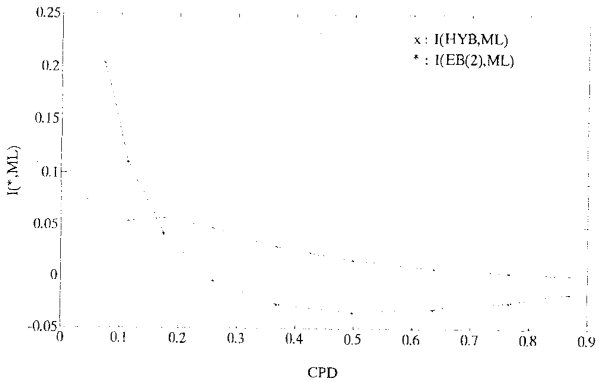

Fig. 4. Improvement over ML of HYB (-x-) and EB(2) (-*-).

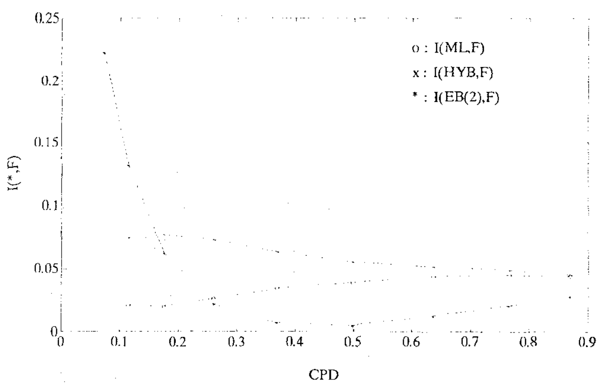

Fig. 5. Improvement over F of ML (-o-), HYB (-x-) and EB(2) (-*-).

of CPD), it is much better than both F and ML. For example, for a CPD of 0.1, the RMSE of EB(2) is smaller than that of either F or ML by about 15% of the quantity being estimated. EB(2) remains reliable for CPD values down to about 0.05 . Hence, its reliable region is larger than that of either F or ML. HYB is better than both F and ML.

IV. CONCLUSIONS

The ML is a uniformly minimum variance unbiased estimator for P, but we have formulated a biased estimator which is better in the MMSE sense. This hybrid estimator combines the estimates from an empirical Bayes estimator and a jackknifed Bayes estimator.

The only paper that we are aware of, which explicitly addresses the problem investigated here, and which suggests an alternative to F for estimating the CPD of surveillance radars is [1]. We now have three competing estimators which may be used instead of F. Their performances are summarized, in terms of their improvements over F, in Fig. 5.

In [1], the construction of exact confidence intervals for F and approximate confidence intervals for ML was also addressed. Since EB(2) and HYB are complex functions of D as well as biased, it is difficult to construct confidence intervals for them. One way to approximate such confidence intervals may be through the use of bootstrap methods [4]. This possibility will be studied in a follow-up investigation.

DOMINIC S. LEE
DANIEL Q. NAIMAN
Mathematical Sciences Department
The Johns Hopkins University
Charles and 34th Sts.
Baltimore, MD 21218

REFERENCES

[1] Rogers, S. R. (1993)
Statistical tests for surveillance radars.
IEEE Transactions on Aerospace and Electronic Systems, **29** (July 1993), 988–994.

[2] Quenouille, M. H. (1956)
Notes on bias in estimation.
Biometrika, **43** (1956), 353–360.

[3] Efron, B., and Morris, C. (1973)
Stein's estimation rule and its competitors—An empirical Bayes approach.
Journal of the American Statistical Association, **68** (Mar. 1973), 117–130.

[4] Efron, B. (1979)
Bootstrap methods: Another look at the jackknife.
Annals of Statistics, **7** (1979), 1–26.

A Multifeature Decision Space Approach to Radar Target Identification

This work focuses on the use of actual radar sensor data to construct a multifeature decision space formulation to the target identification (TID) problem. The decision space concepts are classical and the basic target features used can be extracted from the data provided by standard radar sensor operating modes. The target features used in the decision process along with the construction of a useful statistical description of each feature for a given target are presented. A multidimensional formulation of the decision space and the decision logic is also presented leading to a versatile multifeature based algorithm. The algorithm performance has been evaluated on live data and the results are reported.

I. INTRODUCTION

The importance of having an airborne target identification (TID) capability for military and

Manuscript received March 21, 1994; revised January 9, 1995.

IEEE Log No. T-AES/32/1/00788.

This work was partially supported by the Office of Naval Research under NAWCADWAR Contract N62269-90-C-0514.

0018-9251/96/$5.00 © 1996 IEEE

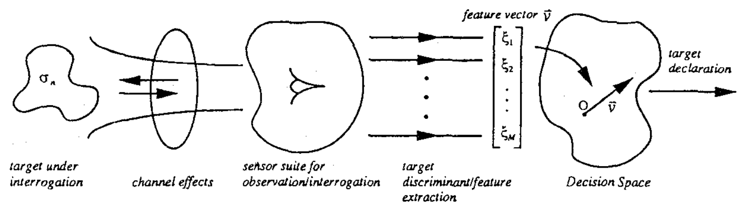

Fig. 1. General model for TID problem.

commercial applications is easily established by considering the Iranian air bus tragedy over the Persian Gulf in 1988 [1]. The task of identifying an airborne target uniquely from radar sensor information is very challenging. It is for this reason that multiple target features are used within a common statistical framework to reliably and robustly provide a usable airborne TID capability. The performance of any statistical identification process that is phenomena driven relies on both the quality of the discriminants as provided by the sensing system, and the correct interpretation of their physical significance.

The general model for the TID problem used in this work is shown in Fig. 1. The model is considered to be general because it can readily accommodate the use of multiple sensors. The sensor suite can be a combination of active, passive, distributed, and colocated sensors that together cover a broad spectral band chosen to exploit a range of target characteristics. In addition, individual channel effects associated with the operation of each sensor must be accounted for in the decision process. The data received by the sensor suite is processed to extract target features using appropriately chosen measures. Many researchers are actively pursuing useful solution concepts addressing different aspects of the general TID problem shown in Fig. 1 [2–4]. Note that target feature extraction is typically the most processing-intensive step of the TID problem, and processor hardware requirements can vary considerably for real-time implementation of different TID solution concepts. The target features extracted from the sensor suite are combined to form a single multi-dimensional feature vector $\vec{v}$. The feature vector is then mapped into a decision space (that resides in computer memory) and a particular target is declared. A classical Bayesian Decision Rule (BDR) is used, and a suitably sized sliding set of declarations can be treated as being made up of independent trials that can be subsequently combined as a Bernoulli experiment [5–7]. However, the Bernoulli trial stage of the decision process is time line driven, and emphasis is appropriately placed on the single trial declaration performance. The statistical confidence of the target declaration is of prime importance, and there are numerous places for error to enter the decision process. For example, decision error can arise from any combination of a poor understanding of target phenomenology, channel effects not taken into account, poor real-time sensor measurement fidelity, poor feature extraction processing performance, and an incorrectly constructed decision space.

The primary thrust of this work focuses on a formidable subset of the TID tsk that involves the use of a single monostatic radar sensor (active and colocated) opening at X-Band. Depending upon the radar's specific operating parameters that include the antenna transfer function, transmit waveform (modulation type, pulse-repetition frequency (PRF), etc.) and coherent burst characteristics, a number of discriminating target features can be extracted from the received data. The use of target features that are not based on high resolution Doppler spectra was of particular interest in this work. The specific target feature baseline consists of target radar cross section (RCS) [8], length, two spectral features extracted from jet engine modulation (JEM) [9], and target velocity and altitude. Together, these features are combined to form a 6-dimensional feature over $\vec{v}$. The subsequent sections describe the data-intensive construction of the decision space that consists of 26 targets, the formation and implementation of the BDR, and the performance obtained from a live target near real-time demonstration. In addition, the combined feature discriminant contribution with statistical description and data integrity are investigated through examining the decision space target partitioning. The relative importance of the different target features in the overall decision process is also examined. Suggestions for additional radar sensor derived discriminants to further enhance TID performance are provided in the concluding remarks.

II. DECISION SPACE CONSTRUCTION

The decision space construction is based on classical concepts that are commonly used in pattern recognition applications. A detailed discussion is given by Fukunaga [5]. This section outlines how these concepts have been applied to the TID problem described in Fig. 1.

To construct an ideal decision space, the elements of the feature vector $\vec{v}$ must together establish disjoint regions to exactly partition the N hypothesis (N is

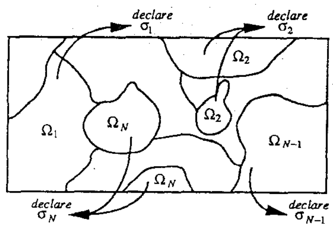

Fig. 2. N-hypothesis TID problem.

TABLE I
Feature Vector Elements (Discriminants) and Their pdfs

Target Feature	Notation	Probability Density Function
RCS	ξ_1	β-density/empirical
length	ξ_2	trapezoidal/empirical
JEM1	ξ_3	trapezoidal/empirical
JEM2	ξ_4	trapezoidal/empirical
velocity	ξ_5	piece-wise uniform/empirical
altitude	ξ_6	piece-wise uniform/empirical

the total number of targets) TID problem. The M element feature vector (M-tuple of real numbers) is defined as $\vec{v} = [\xi_1\ \xi_2\ \cdots\ \xi_M]^T$ where each of the ξ_m represents a particular target discriminant. For the TID problem, let the outcome Ω_n correspond to a declaration "target σ_n" with a probability $P(\sigma_n)$ where the subscript n denotes the nth target out of the possible $\{\sigma_n;\ n = 1,\ldots,N\}$. The classical model for this situation is shown in Fig. 2.

Utilizing the elements of the feature vector explicitly, the Ω_n outcome can be expressed as the joint intersection given by

$$\Omega_n = \left(\bigcap_{m=1}^{M} \Omega_n^{\xi_m}\right) \tag{1}$$

where $\Omega_n^{\xi_m}$ are the individual outcomes resulting from each of the target discriminants ξ_m. The overall quality of the decision space resulting from the set of features contained in $\vec{v}$, and the value added provided by the inclusion of each ξ_m should be statistically quantified, and for some targets

$$\Omega_n = \left(\bigcap_{m=1}^{M} \Omega_n^{\xi_m}\right) = \left(\bigcap_{m=1}^{M'} \Omega_n^{\xi_m}\right); \qquad M' < M. \tag{2}$$

The value of each discriminant ξ_m in the TID decision process implied by condition (2) is important when selecting useful discriminants, and deciding appropriate feature weighting schemes to exploit the relative importance of individual features for a particular target. To allow importance weighting to be utilized, conditional decision subspaces must be constructed whose members are of equal importance.

The decision space (or decision subspace) construction requires individual statistical descriptions of each discriminant ξ_m in the feature vector, and consequently requires the formulation of a joint probability density function (pdf) for each target. From practical considerations the individual target features are assumed to be independent and the conditional feature vector pdfs $f_{\sigma_n}(\vec{v} \mid \sigma_n)$ for each target take the form

$$\begin{aligned}
f(\vec{v} \mid \sigma_1) &= f_{\sigma_1}(\vec{v}) = f_{\sigma_1}(\xi_2)\cdots f_{\sigma_1}(\xi_M) \\
&= \prod_{m=1}^{M} f_{\sigma_1}(\xi_m) \\
f(\vec{v} \mid \sigma_2) &= f_{\sigma_2}(\vec{v}) = f_{\sigma_2}(\xi_2)\cdots f_{\sigma_2}(\xi_M) \\
&= \prod_{m=1}^{M} f_{\sigma_2}(\xi_m) \\
&\vdots \\
f(\vec{v} \mid \sigma_N) &= f_{\sigma_N}(\vec{v}) = f_{\sigma_N}(\xi_2)\cdots f_{\sigma_N}(\xi_M) \\
&= \prod_{m=1}^{M} f_{\sigma_N}(\xi_m)
\end{aligned} \tag{3}$$

where the ξ_m have different conditional pdfs $f_{\sigma_n}(\xi_m)$, some of which may not have parametric forms. Note that joint statistical independence among the ξ_m is a valid assumption based on physical and practical considerations. The generalized decision space is constructed from the N conditional M-dimensional pdfs given by (3) for the case of equally important elements of the feature vector.

The decision space details that remain pertain directly to the $\{\xi_m : m = 1,\ldots,M\}$ and their corresponding pdfs for the total number of targets in the data base. The decision space constructed for this work contains a combination of commercial and military aircraft totaling $N = 26$ targets. Each target is characterized using $M = 6$ independent discriminants. The target discriminants and their corresponding pdfs are listed in Table I. The RCS discriminant is constructed from compiled measured data, and can be expressed parametrically as a β-density [8]. The JEM1 and JEM2 discriminants are based on spectral features extracted from jet engine modulation signatures, and each are taken have trapezoidal densities that are parameterized for individual targets using previously measured and analyzed JEM spectrum data. The target length discriminant is taken to have a trapezoidal distribution that is parameterized using known physical information. The velocity and altitude discriminants are assumed to have piece-wise uniform distributions that are parameterized from operational data.

III. BAYESIAN DECISION RULE FORMULATION

The decision rule for the TID problem is classical and detailed discussions can be found in many texts (e.g. [5]). Using total probability and Bayes' Theorem for equally important feature vector elements, the decision rule follows from maximizing the probability

$$P(\sigma_n \mid \vec{v}^s) = \frac{f(\sigma_n, \vec{v}^s)}{f(\vec{v}^s)} = \frac{P(\sigma_n) f_{\sigma_n}(\vec{v}^s)}{f(\vec{v}^s)} \tag{4}$$

for some $n = i$ to declare σ_i, where

$$f(\vec{v}^s) = \sum_{n=1}^{N} P(\sigma_n) f_{\sigma_n}(\vec{v}^s) \tag{5}$$

is a constant. Note that $\vec{v}^s$ designates a particular feature vector $\vec{v}$ measured by the sensing system. Equation (5) implies that events Ω_n that correspond to declarations σ_n partition the decision space. From (4) the BDR can be expressed explicitly as

$$\max_n (P(\sigma_n) f_{\sigma_n}(\vec{v}^s)) \rightarrow \Omega_1 \Rightarrow \text{declare } \sigma_i \tag{6}$$

where the maximization of $P(\sigma_n) f_{\sigma_n}(\vec{v}^s)$ occurs for some $n = i$ indicating the event Ω_i, and corresponds to declaring target σ_i. Note that single outcome evaluation of (6) is straight forward, and in practice it is desirable to rank all possible target declarations in decreasing probability. Thus, (6) can be repeatably evaluated a total of $N - 1$ times where successive computations omit previous declarations. When relative importance weighting among the elements of the feature vector is utilized, separate decision rules must be formulated for each decision subspace. The steps are identical to the case of equal importance weighting except that a partitioned feature vector is used (see [5] for more details).

IV. ALGORITHM IMPLEMENTATION AND RESULTS

The TID algorithm was implemented according to (6) with $P(\sigma_n) = N^{-1}$ and demonstrated in near real-time using an airborne AWG-10 (APG-59) radar system operated on a rooftop at the Naval Air Warfare Center Aircraft Division, Warminster, PA in September 1993. The AWG-10 is a high PRF pulse Doppler X-Band radar system that has undergone modifications to provide access to radar signal and tracking information. In addition, external circuitry to perform target length measurement using the leading and trailing edge of the radar return was developed. The TID algorithm is hosted on a 486-PC that accepts radar information via 3 analog-to-digital (A/D) converter boards. In addition, the 486-PC also controls data collection to allow time-on-target and frame time to match the coherent processing interval (CPI) of typical surveillance or tracking radars. For the results presented in this work the radar was operating at a PRF = 300 KHz with a time-on-target of 8 ms within a frame time of 100 ms that was repeated for 5 s defining a single CPI. The CPI of the radar is illustrated schematically in Fig. 3. A live TID demonstration was conducted with a cooperative

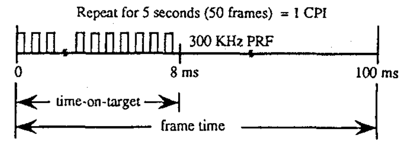

Fig. 3. AWG-10 radar CPI for near real-time TID demonstration.

TABLE II
TID Algorithm Performance for an F-18 Aircraft

Rank	Percentage of 29 CPIs
Top 1	3 %
Top 2	7 %
Top 3-4	24 %
Top 5	62 %
Top 6	90 %
Top 7-8	97 %
Top 9-13	100 %

F-18 aircraft. The duration of the target engagement consisted of 29 consecutive CPIs.

Note that because of the high PRF and the radar and stepped-frequency waveform limitations, the target length measurement required additional circuitry and a separate measurement using the 1 KHz pulse mode of the AWG 10. Unfortunately, the required length measurement circuitry was not working properly during the near real-time demonstration, and was unavailable for inclusion in the feature vector and subsequent TID processing. Thus, all results are based on $\vec{v} = [\xi_1 \bullet \xi_3\ \xi_4\ \xi_5\ \xi_6]^T$, i.e., the use of ξ_2 is omitted. In addition, the radar was also suffering some intermittent FM ranging problems that caused radar data corruption. However, despite hardware difficulties very good live results were obtained for a high percentage of CPIs. The overall results for an F-18 aircraft are summarized in Table II where the performance of the algorithm is determined by a percentage of 29 CPIs corresponding to a particular ranking within the decision space. Note that the results shown in Table II must be interpreted carefully, and were intentionally compiled to illustrate a conservative performance picture of the TID decision space/algorithm. Inspection of the individual CPI results suggest that the Bayes error (decision space distance) between the F-18 aircraft discriminant pdfs and the corresponding adjacent incorrect declaration pdfs are relatively small, i.e., the ranking in Table II shows groupings where aircraft declarations were comparable for that percentage of the 29 CPIs. For example, the Top 6 ranking corresponds to the F-18 aircraft being among the 6 aircraft (out of the 26 aircraft) identified 90% of the time. Rankings in Table II correspond to cases where the feature vector, when projected into the decision space, falls into regions where the distinction between adjacent target declarations is difficult to resolve.

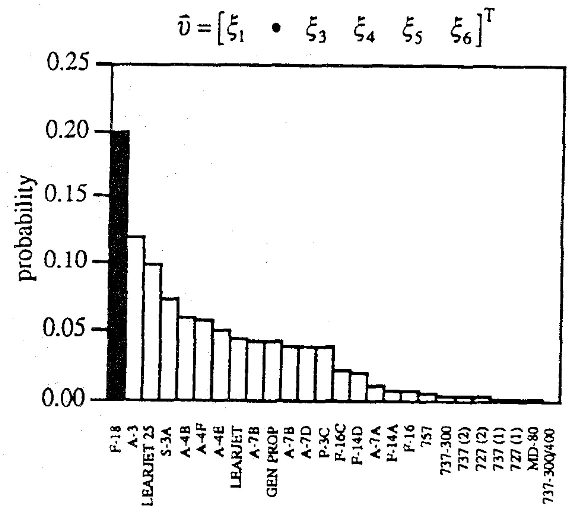

Fig. 4. Near real-time correct identification of an F-18 aircraft.

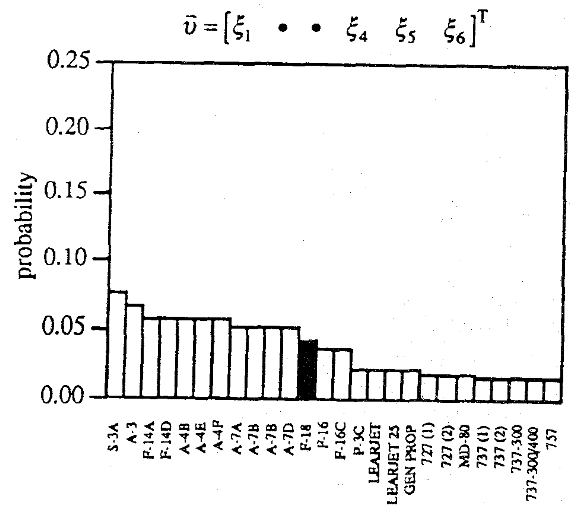

Fig. 6(a). Target JEM1 omitted from feature vector.

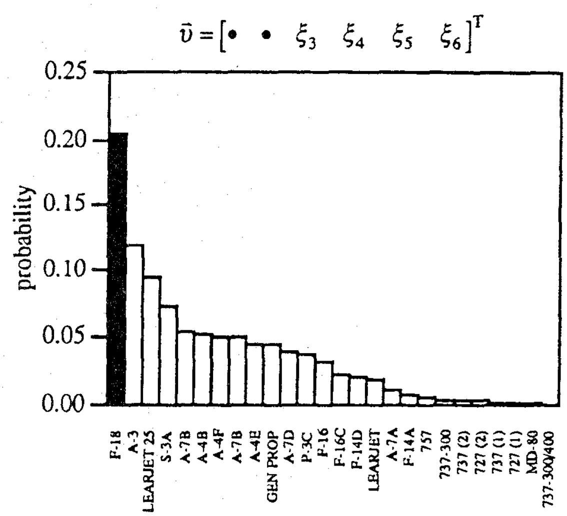

Fig. 5(a). Target RCS omitted from feature vector.

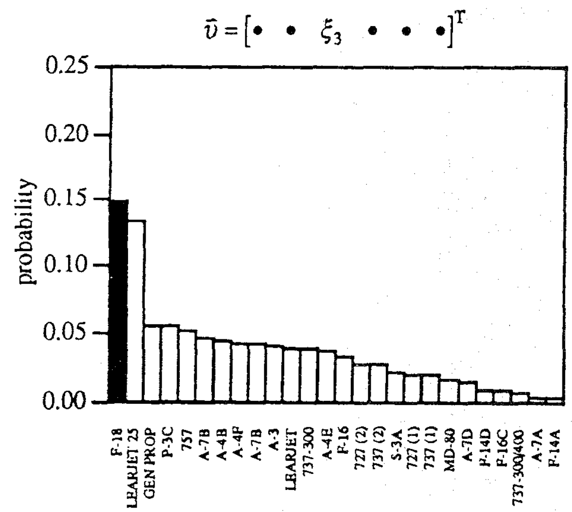

Fig. 6(b). TID performance using only JEM1 information.

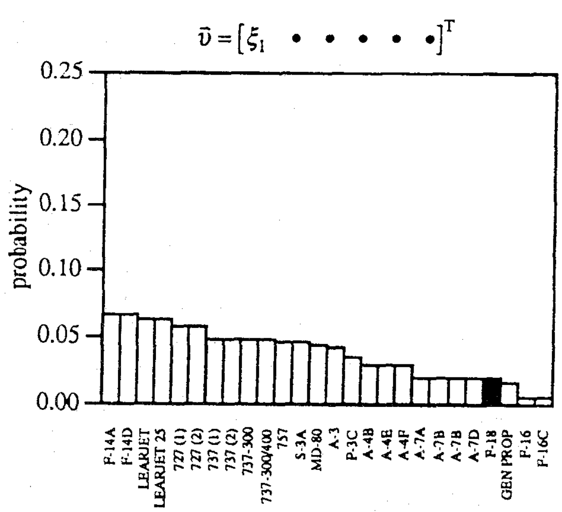

Fig. 5(b). TID performance using only RCS information.

The use of decision space pdfs with better fidelity in combination with appropriate importance weighting (a priori probabilities) among the elements of the feature vector would lead to improved performance. The 3% result is shown in Fig. 4 where the F-18 aircraft is shown highlighted along with the remaining 25 aircraft in the decision space.

Figs. 5–9 illustrate the performance of the algorithm with respect to each discriminant in the feature vector along with the complimentary set of discriminants for the F-18 aircraft result in Fig. 4. For all results marginal pdfs are used to examine the performance associated with the individual components of the feature vector (this situation is represented by (2)). For example, Fig. 5(a) shows the TID performance without the use of RCS information, and Fig. 5(b) shows the TID performance using only RCS information for the F-18 aircraft. Note

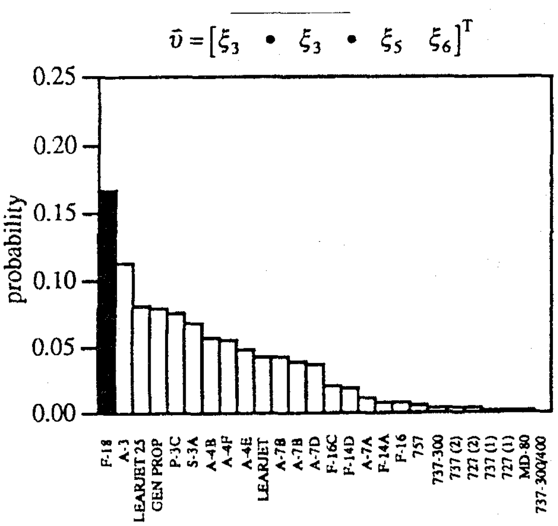

Fig. 7(a). Target JEM2 omitted from feature vector.

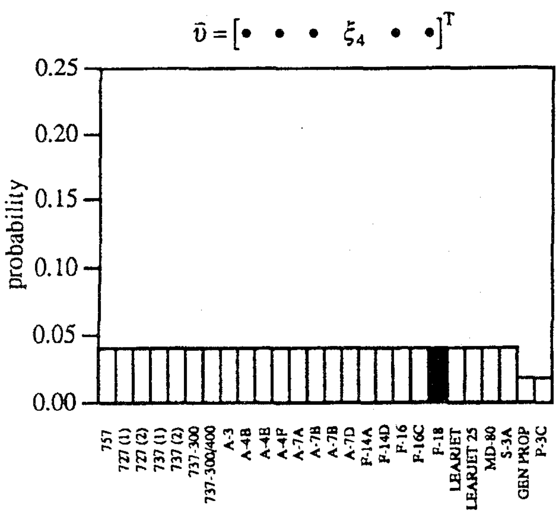

Fig. 7(b). TID performance using only JEM2 information.

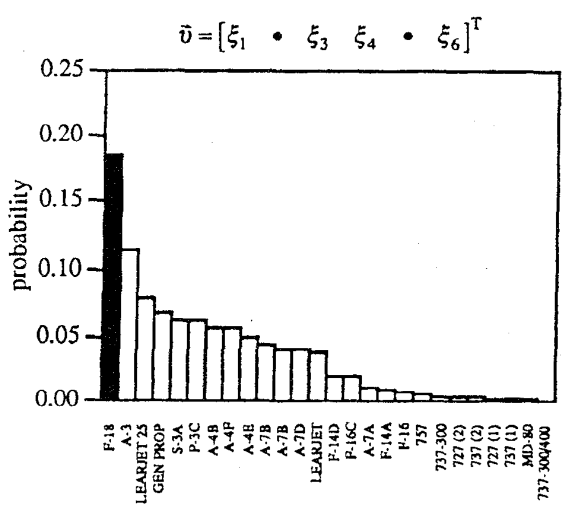

Fig. 8(a). Target velocity omitted from feature vector.

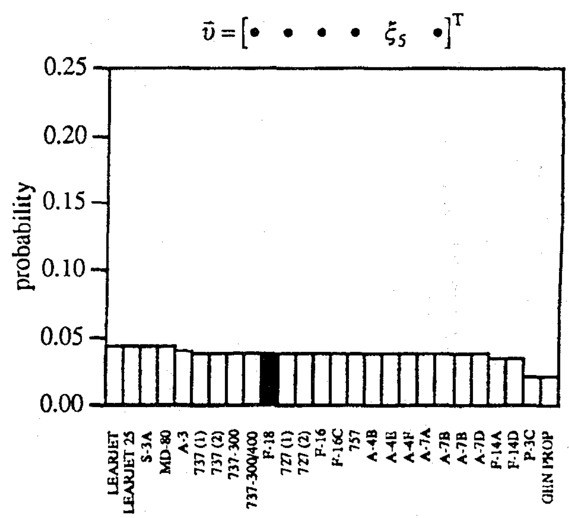

Fig. 8(b). TID performance using only velocity information.

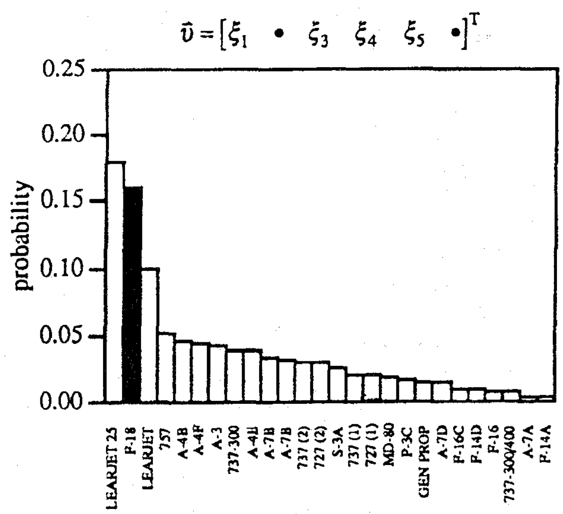

Fig. 9(a). Target altitude omitted from feature vector.

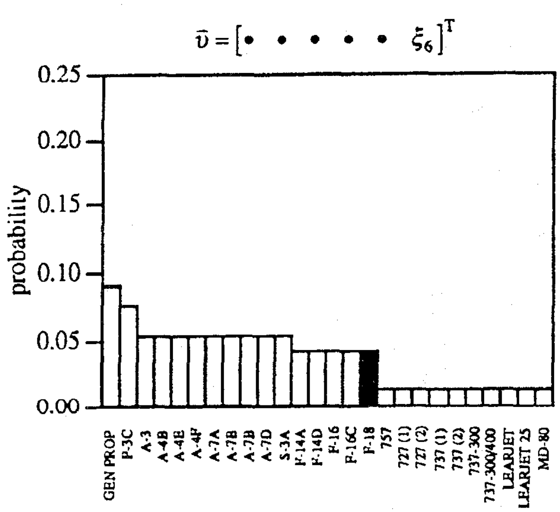

Fig. 9(b). TID performance using only altitude information.

that after the demonstration, it was determined that radar calibration errors and FM ranging problems were inhibiting the value of RCS information in TID algorithm. Off-line reprocessing is expected to show performance improvement over the result given in Fig. 5(b). Figs. 6(a) and (b) illustrate the TID results for JEM1. Fig. 6(b) indicates that JEM1 appears to be a good discriminant for an F-18. Figs. 7(a) and (b) illustrate the TID results for JEM2. Fig. 7(b) indicates that JEM2 was not a high value discriminant for F-18 identification. This result is not surprising because the primarily value of JEM2 is to distinguish jet versus propeller engine types. Figs. 8(a) and (b) illustrate the TID results for target velocity. Fig. 8(b) indicates that velocity information played a minor role in identifying the F-18 aircraft. Note that Fig. 8(b) does not necessarily devalue velocity information for F-18 aircraft identification. The results simply indicate that for this engagement, velocity did not play a significant role in the TID algorithm performance. Figs. 9(a) and (b) illustrate the TID results for target altitude. Fig. 9(b) indicates that altitude had a modest role in the F-18 identification where a distinct separation between military and commercial aircraft was obtained.

V. CONCLUSIONS

The TID problem has been treated as a generalized multidimensional decision process based on statistical representations of target discriminants that are observed by a sensor or sensor suite. The classical BDR formulation is extremely versatile and can readily accommodate a large number of discriminants [5]. In addition, the basic target discriminant information (pdfs) can be augmented with target and/or situation dependent a priori importance weighting that is either fixed or adaptive to enhance TID performance. The TID algorithm has been tested in real-time using a modified AWG10 radar with selected target discriminants that can be extracted from CPIs that are typical of modern surveillance and tracking radars. The testing portion of this work served to both validate the multifeature decision space algorithm, and examine the quality of a basic set of target discriminants. The live TID algorithm performance with the selected target discriminants is very modest, but encouraging despite the hardware difficulties. (In particular, the Top 6 ranking in Table II corresponds to the F-18 aircraft being among the 6 out of the 26 aircraft identified 90% of the time.) Examination of the benefit provided by the individual discriminants show that expected performance can deviate significantly from what is achieved in actual target engagement scenarios. The overall results clearly indicate the need for better target discriminants. The appropriate selection of target discriminants is generally driven by the limitations of the sensing system. For radar sensors, the use of sophisticated discriminants generally requires the combination fo waveform selection and specialized processing to exploit particular target scattering characteristics. For example, target RCS as a function of carrier frequency and angle of illumination is a relatively basic case [10]. Highly analytical research in target scattering phenomenology indicates that target natural resonance extraction [11] and polarimetric signatures [12] are excellent target discriminants. Furthermore, information extraction techniques that are optimally matched to nonstationary target characteristics are also likely to play a role in the selection and refinement target discriminants [13]. In all cases, the generalized multifeature decision space approach presented here allows target discriminants to be utilized within a single unified TID algorithm.

ACKNOWLEDGMENT

The authors appreciate the efforts of Mr. D. Davis, Mr. J. Lytle, Mr. V. Colon, Mr. B. Wohlers, Mr. A. Swanson, Mr. T. Coyle, Mr. D. Mulholland, Mrs. D. Howry, and Mr. D. Abassi for contributing to the overall success of the TID demonstration.

J. G. TETI, JR.
R. P. GORMAN
JJM Systems, Inc.
530 West Street Rd.
Suite 200
Warminster, PA 18974

W. A. BERGER
Dept. of Physics and Electronics Engineering
University of Scranton
Scranton, PA

REFERENCES

[1] Jaska, P. R. (1988)
AEGIS system still gets high marks.
Defense Electronics, **20**, 11 (Oct. 1988).

[2] Leung, D. S. P., and Williams, D. S. (1991)
A multiple hypothesis based multiple sensor spatial data fusion algorithm.
SPIE Automatic Object Recognition, **1471** (1991).

[3] Sims, S. R. F., and Dasarathy, B. V. (1992)
Automatic target recognition using a passive multisensor suite.
Optical Engineering, **31**, 12 (Dec. 1992).

[4] Thomopoulos, S. C. A., Viswanathan, R., and Bougoulias, D. C. (1987)
Optimal decision fusion in multiple sensor systems.
IEEE Transactions on Aerospace and Electronic Systems, **AES-23**, 5 (Sept. 1987).

[5] Fukunaga, K. (1968)
Introduction to Statistical Pattern Recognition.
New York: Wiley, 1968.

[6] Van Trees, H. L. (1990)
Detection, Estimation, and Modulation Theory, Part 1.
New York: Academic Press, 1990.

[7] Papoulis, A. (1984)
Probability, Random Variables, and Stochastic Processes.
New York: McGraw-Hill, 1984.

[8] Maffett, A. L. (1989)
Topics for a Statistical Description of Radar Cross Section. New York: Wiley, 1989.

[9] Bell, M. R., and Grubbs, R. A. (1993)
JEM modeling and measurement for radar target identification.
IEEE Transactions on Aerospace and Electronic Systems, **29**, 1 (Jan. 1993).

[10] Snorrason, O., and Garber, F. D. (1992)
Evaluation of nonparametric discriminant analysis techniques for radar signal feature selection and extraction.
Optical Engineering, **31**, 12 (Dec. 1992).

[11] Baum, C. E., Rothwell, E. J., Chen, K.-M., and Nyquist, D. P. (1991)
The singularity expansion method and its application to target identification.
Proceedings of the IEEE, **79**, 10 (Oct. 1991).

[12] Boerner, W.-M., Yan, W.-L., Xi, A.-Q., and Yamaguchi, Y. (1991)
On the basic principles of radar polarimetry: The target characteristic polarization state theory of Kennaugh, Huynen's polarization fork concept, and its extension to the partially polarized case.
Proceedings of the IEEE, **79**, 10 (Oct. 1991).

[13] Teti, J. G., Jr. (1994)
Weyl-Heisenberg and wavelet phase space filtering using waveform signature templates.
In *SPIE International Symposium Digest—Wavelet Applications*, **2242**, Orlando, FL, Apr. 4–8, 1994.

A General Approach to TMA Observability from Angle and Frequency Measurements

The state-observability problem for passive target tracking by angle and/or frequency measurements is analyzed. The method used is independent of the target model and can be specialized to arbitrary models in a systematic way. As an example, the general Nth-order dynamics target model has been discussed. In this way the previously established necessary and sufficient observability conditions are rederived in a much simpler way and extended to more general cases.

I. INTRODUCTION

Passive emitter state estimation (commonly referred to as target motion analysis (TMA)) is a widely investigated problem of practical interest. A particular interesting case arises when all measurements are derived from a single moving observer. Suitable data are in principle all measurements which are functions of the target state. In this work the observer-to-target angles and the Doppler-shifted emitter frequency are considered.

A basic requirement for TMA is system observability, i.e., the existence of a unique tracking solution. If only angle measurements are available, it is well known that target state observability is warranted only under specific conditions. The conditions change, if other types of data (e.g., the Doppler-shifted signal frequency) are used. In practice, precise knowledge of these conditions is of fundamental importance since reliable estimations can be obtained only if the target state is completely observable.

In the literature the observability problem from angle and frequency measurements has been discussed in several papers. All papers start from a finite dynamics target model and differ by the method used or by the degree of target dynamics.

In case of angle measurements only, two essentially different approaches to the solution of the TMA observability problem have been made. The first takes advantage of the fact that the system though intrinsically nonlinear can be recast in linear form which allows direct application of theorems from the well-known classical theory of observability in linear systems. In this way the constant velocity target (first-order dynamics) case has been studied in detail in two [1] and three [2] dimensions. The specific observability criterion thereby used, however, leads to complicated nonlinear differential equations. Some tedious mathematics are needed for the solution, giving conditions that are necessary for system observability. Starting from another but equivalent criterion complicated nonlinear differential equations can be avoided. This was done in [3–5], yielding necessary and sufficient observability conditions for two-dimensional first-order [3], three-dimensional second-order [4], and general three-dimensional Nth-order [5] dynamics targets, respectively.

The second approach avoids analyzing an observability matrix and solves the observabilty problem for the general three-dimensional Nth-order dynamics target case via establishing an equivalent uniqueness criterion for an associated functional equation [6].

Observability from the combined set of angle and frequency measurements has been investigated in [4, 7, and 8]. As in the case of angle measurements only, the nonlinear equations can be recast in linear form by a judicious choice of variables. Based on the criterion used in [3–5], necessary and sufficient observability conditions have been established for two-dimensional first-order dynamics targets and stationary observers.

If only frequency measurements are available the system equations cannot be recast in equivalent linear form. The nonlinearities suggest an observability analysis based on the Jacobian matrix of the pertinent

Manuscript received July 20, 1994; revised April 24, 1995.

IEEE Log No. T-AES/32/1/00790.

0018-9251/96/$5.00 © 1996 IEEE